

Analysis by a Finite Element Hybrid Method," 3rd Conference on Matrix Methods in Structural Mechanics, Wright-Patterson Air Force Base, Ohio, Oct. 19-21, 1971.

¹⁴ Dugan, R., Severn, R. T., and Taylor, P. R., "Vibration of Plate and Shell Structures Using Triangular Finite Elements," *Journal of Strain Analysis*, Vol. 2, No. 1, Jan. 1967, pp. 73-83.

¹⁵ Lundgren, H. R., "Buckling of Multilayer Plates by Finite Elements," Ph.D. thesis, 1967, Oklahoma State Univ., Stillwater, Okla.

¹⁶ Henshell, R. D., Neale, B. K., and Warburton, G. B., "A New Hybrid Cylindrical Shell Finite Element," *Journal of Sound and Vibration*, Vol. 16, No. 4, 1971, pp. 519-531.

¹⁷ Washizu, K., "Note on the Principle of Stationary Complementary Energy Applied to Free Vibration of an Elastic Body," *International Journal of Solids and Structures*, Vol. 7, No. 3, 1971, pp. 251-268.

¹⁸ Sakaguchi, R. L. and Tabarrok, B., "Calculations of Plate Frequencies from Complementary Energy Formulations," *International Journal of Numerical Methods in Engineering*, Vol. 2, 1970, pp. 430-451.

¹⁹ Tabarrok, B., "A Variational Principle for the Dynamic Analysis of Continua by Hybrid Finite Element Method," *International Journal of Solids and Structures*, Vol. 7, No. 3, March 1971, pp. 251-268.

²⁰ Toupin, R. A., "A Variational Principle for the Mesh-Type Analysis of a Mechanical System," *Journal of Applied Mechanics*, Vol. 76, No. 1, Jan. 1952, pp. 151-152.

²¹ Icnaczak, J., "A Completeness Problem for Stress Equations of Motion in the Linear Elasticity Theory," *Archivum Mechaniki Stosowanej*, Vol. 15, No. 2, 1951, p. 225.

²² Gurtin, M. E., "Variational Principles for Linear Elastodynamics," *Archive for Rational Mechanics and Analysis*, Vol. 16, No. 1, 1964, pp. 36-50.

²³ Fried, I., "Finite Element Analysis of Time Dependent Phenomena," *AIAA Journal*, Vol. 7, No. 6, June 1970, pp. 1170-1172.

²⁴ Mikusinski, J., *Operational Calculus*, Pergamon Press, New York, 1959, pp. 28-56.

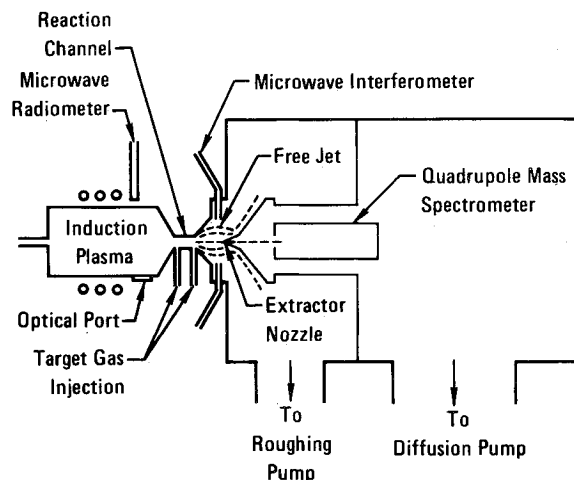


Fig. 1 Experimental apparatus.

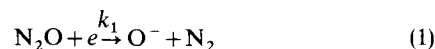
transit time is dependent on both the channel length and the gas temperature. The species formed in the channel are "chemically frozen" by a rapid freejet expansion into a low-pressure, high-mass-flow vacuum system resulting in a 300-fold pressure reduction. This results in a five orders of magnitude decrease in the rate of product formation, since the rate of product formation is proportional to the product of the reactant number densities if reaction cross sections are assumed to remain constant.

A K_a band microwave interferometer is used to measure the electron density in the expansion region nine-channel-diameters downstream of the channel exit plane. Electron densities at the interferometer range from 10^{11} – 10^{13} cm^{-3} . This corresponds to electron densities in the reaction channel of 3×10^{13} to 3×10^{15} cm^{-3} .

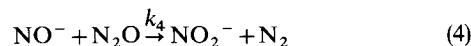
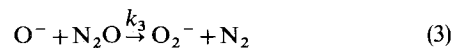
Tungsten-tungsten 75%, rhenium 25%—thermocouples inserted in the reaction channel are used to measure the reaction channel gas temperature. Gas temperatures in the channel have also been measured spectroscopically using radiation from rotational excitation of diatomic molecules.²

2 Assumptions and Basic Equations

Chemical reactions are assumed to occur only in the reaction channel downstream of the point of target gas injection. Reaction products are sampled from the freejet through a conical extractor into a high vacuum (10^{-6} torr) region for analysis with a quadrupole mass spectrometer.³ Results of previous investigations of negative ion formation mechanisms with N_2O target molecules at high gas temperatures (2000–3000°K) using this apparatus have shown dissociative electron attachment to be the primary process.⁴ For short reaction times the principal product is formed according to



For longer reaction times, however, additional reactions are necessary to account for the presence of additional negative ions.³ A reaction sequence which would describe the observed ions when coupled with Eq. (1) is



This Note compares the predicted O^- intensities using a binary collision model with the O^- intensities measured mass spectrometrically using three 50- μm -diam flush-mounted supersonic

Ion Intensity Measurement in a Plasma Reaction Channel

J. H. MULLEN,* J. M. MADSON,* AND L. N. MEDGYESI-MITSCHANG*

McDonnell Douglas Research Laboratories, McDonnell Douglas Corporation, St. Louis, Mo.

1 Introduction

THIS Note reports the measurement of negative ions formed when N_2O target molecules react with a flowing high temperature argon plasma in a reaction channel. The experimental arrangement shown in Fig. 1 has been described in detail elsewhere.¹ An argon induction plasma is formed in the discharge chamber with a 0-70 kw, 550 kHz, rf generator and expanded into a sonic reaction channel where the gas temperature is in the range of 2000° to 3000°K. Target gas molecules injected into the reaction channel in concentrations of 10^{-3} to 10^{-2} mole fraction of the argon are collisionally heated to the local argon gas temperature in the channel. At normal channel pressures (10-80 torr) the target molecules reach thermal equilibrium in less than 1 μsec and react with the argon plasma during their transit through the reaction channel. Typical transit times in the channel are of the order of 10 μsec . The

Presented as Paper 72-675 at the AIAA 5th Fluid and Plasma Dynamics Conference, Boston, Mass., June 26-28, 1972; submitted August 2, 1972; revision received December 26, 1972. This research was conducted under the McDonnell Douglas Independent Research and Development Program.

Index categories: Atomic, Molecular, and Plasma Properties; Thermochemistry and Chemical Kinetics; Reactive Flows.

* Scientist.

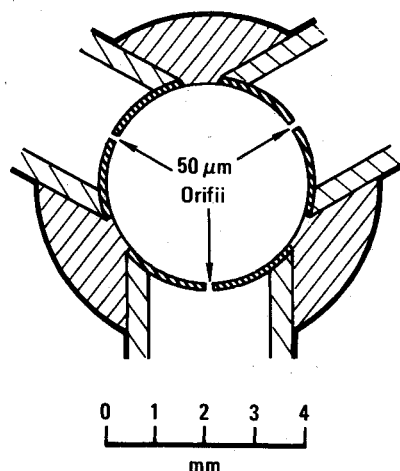


Fig. 2 Flush-mounted supersonic injectors.

target gas injectors shown in Fig. 2. In the reaction model, binary collisions are assumed to be predominantly responsible for the formation of the negative ions. The rate constants are taken to be independent of the reactant and product concentrations, and are time invariant but strongly temperature dependent. In addition, the reactant concentrations are taken to be uniform across the channel and the reaction time proportional to the channel transit time.

The rate equations corresponding to the sequence of reactions for the formation of negative ions are

$$d[\text{O}^-]/dt = [\text{N}_2\text{O}]\{k_1[e] - (k_2 + k_3)[\text{O}^-]\} \quad (5)$$

$$d[\text{NO}^-]/dt = [\text{N}_2\text{O}]\{k_2[\text{O}^-] - k_4[\text{NO}^-]\} \quad (6)$$

$$d[\text{O}_2^-]/dt = [\text{N}_2\text{O}][\text{O}^-] \quad (7)$$

$$d[\text{NO}_2^-]/dt = k_4[\text{N}_2\text{O}][\text{NO}^-] \quad (8)$$

where

$$[\text{N}_2\text{O}] = [\text{N}_2\text{O}]_0 - [\text{O}^-] - [\text{NO}^-] - [\text{O}_2^-] - [\text{NO}_2^-]$$

The three-body collisional radiative recombination theory of Biberman et al.⁵ was used to include the ionization and

recombination effects of the argon plasma in the reaction channel. This approach allows a wide range of plasma conditions in the reaction region to be considered, including departures from local thermodynamic equilibrium as well as possible departures from Maxwellian velocity distributions of the free electrons. To account for argon recombination and ionization one must include the following additional rate equation

$$d[e]/dt = -\alpha(T_e)[e]^3 + \beta(T_e)[\text{Ar}][e] - k_1[e][\text{N}_2\text{O}] \quad (9)$$

The recombination and ionization coefficients α and β , respectively, are functions of the electron temperature T_e of the plasma. These rate equations, Eqs. (5-9), coupling the background argon plasma and the target molecules, can be solved using numerical methods such as the Runge-Kutta or the Hamming modified predictor-corrector methods.

This model has been applied to reactions of N_2O with an argon plasma for a range of temperatures of 2000° to 3000°K. The calculated O^- formation using this model is given as a family of curves with a parameter a . The parameter $a (= k_1[\text{N}_2\text{O}]_0\tau)$ represents the normalized rate constant for the dissociative electron attachment reaction, expressed in terms of the initial electron density $[\text{N}_e]_0$ and the total reaction time τ . Figure 3 shows experimental data along with theoretically predicted values for $a = 1, 2$, and 5.

Interpretation of the experimental results requires knowledge of the target gas concentration in the channel. The uniformity in target gas concentration at any cross section of the reaction channel depends on the degree of mixing of the target gas with the flowing argon plasma. Target gas molecules are injected into the reaction channel supersonically through orifices contoured to the inside channel to present a smooth wall surface to the flowing plasma. Calculations based on the theory for supersonic injection by Orth and Funk⁶ and Billig et al.,⁷ indicate that the target gas penetrates the flowing plasma to a depth equal to the channel radius by the time the end of the channel is reached. Furthermore, measurements of ion intensities and electron density as well as visual observations gave no indication of flow separation which has been observed with protruding subsonic injectors.⁸

3. Conclusions

Target gas injectors that are flush mounted with the reaction channel wall present a smooth boundary to the plasma flow and preserve its uniform characteristics in the channel. Supersonic injection provides good penetration of the target gas into the flowing plasma and results in observed O^- concentrations which agree with the predicted concentrations for a value of the normalized rate constant $a = 2$ as shown in Fig. 2. The $a = 2$ curve of Fig. 2 corresponds to an electron attachment rate constant of $1.3 \times 10^{-10} \text{ cm}^3 \text{ molecule}^{-1} \text{ sec}^{-1}$.

References

- Mullen, J. H., Madson, J. M., Medgyesi-Mitschang, L. N., Peng, T. C., and Doane, P. M., "Apparatus for the Measurement of High Temperature Plasma Reactions," *Review of Scientific Instruments*, Vol. 41, 1970, pp. 1746-1754.
- Medgyesi-Mitschang, L. N. and Hefferlin, R. A., "Characteristics of an Argon rf Plasma: Active Discharge and Laminar Sonic Flow Region," *Journal of Quantitative Spectroscopy & Radiative Transfer*, Vol. 12, 1972, pp. 1627-1639.
- Madson, J. M., Mullen, J. H., and Medgyesi-Mitschang, L. N., "Formation of O^- From N_2O at Temperatures above 2000°K," 19th Annual Conference on Mass Spectrometry and Allied Topics, Atlanta, Ga., May 1971.
- Mullen, J. H., Madson, J. M., and Medgyesi-Mitschang, L. N., "Measurement of Electron Attachment Processes in a High Temperature Plasma," *Proceedings of the IEEE*, Vol. 59, 1971, pp. 605-607.
- Biberman, L. M., Yakubov, I. T., and Vorob'ev, V. S., "Kinetics of Collisional-Radiation Recombination and Ionization in Low Temperature Plasma," *Proceedings of the IEEE*, Vol. 59, 1971, pp. 555-572.

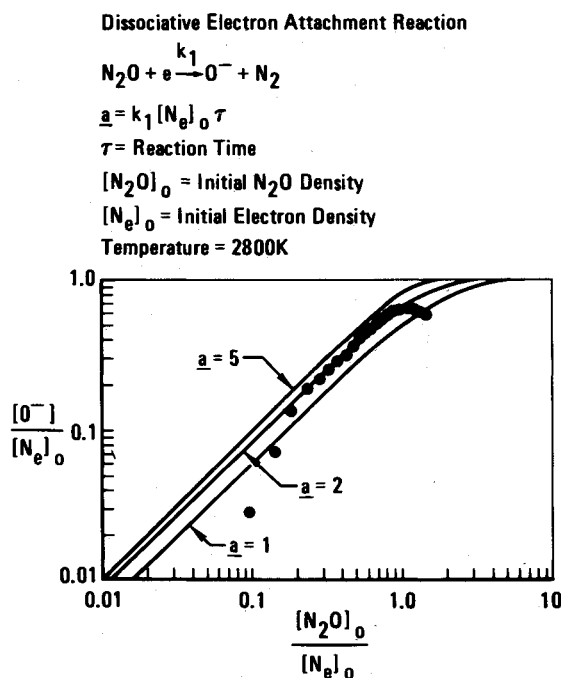


Fig. 3 Comparison of experimental data with theoretically predicted O^- production.

⁶ Orth, R. C. and Funk, J. A., "An Experimental and Comparative Study of Jet Penetration in Supersonic Flow," *Journal of Spacecraft and Rockets*, Vol. 4, No. 9, Sept. 1967, pp. 1236-1242.

⁷ Billig, F. S., Orth, R. C., and Lasky, M., "A Unified Analysis of Gaseous Jet Penetration," *AIAA Journal*, Vol. 9, No. 6, June 1971, pp. 1048-1058.

⁸ Mullen, J. H., Madson, J. M., and Medgyesi-Mitschang, L. N., "Ion Intensity Measurement in a Plasma Reaction Channel," *AIAA Paper 72-675*, Boston, Mass., 1972.

Coupled Thermally Induced Vibrations of Beams

A. G. SEIBERT*

Hamilton Standard Division, United Aircraft Corporation,
Windsor Locks, Conn.

AND

J. S. RICE†

Materials Sciences Corporation, Blue Bell, Pa.

Introduction

THE field equations for coupled thermoelastic vibrations of Rayleigh and Timoshenko beams¹ have been derived by Jones.² Boley and Barber investigated thermally induced flexural vibration of a simply supported Bernoulli-Euler beam due to heat input to one edge of the span using the one-dimensional heat conduction equation.³ This Note compares thermally induced vibrations of a simply supported beam with heat input to one edge for Bernoulli-Euler and Timoshenko beams when the field equations with one-dimensional heat conduction are thermoelastically coupled and uncoupled; and for the uncoupled case of two-dimensional heat conduction. The latter analysis shows that a step heat input may cause significant vibrations in short beams as well as long beams.

The Timoshenko beam: thermoelastically coupled vibrations

Considering flexural vibrations the basic equations

$$k \oint x \frac{\partial \theta}{\partial n} ds + k \tilde{\theta}_{y,zz} - c_0 \tilde{\theta}_{y,t} - \frac{kA}{I_{yy}} \tilde{\theta}_y = -\beta_0 T I_{yy} u_{,zzt} + \beta_0 \frac{T I_{yy} \rho}{K_x \mu} u_{,tt} \quad (1a)$$

$$EI_{yy} u_{,zzzz} + \rho A u_{,tt} - \left(\rho I_{yy} + \frac{EI_{yy} \rho}{K_x \mu} \right) u_{,zzt} + \frac{\rho^2 I_{yy}}{K_x \mu} u_{,ttt} + \beta_0 \tilde{\theta}_{y,zz} = 0 \quad (1b)$$

can be obtained from Jones² except for the integral

$$k \oint x (\partial \theta / \partial n) ds = -qh/2 \quad (2)$$

which accounts for the heat input to one edge of the beam. In Eqs. (1) and (2), a comma followed by a subscript denotes partial differentiation with respect to the subscript, E is Young's modulus, α is the thermal coefficient of linear expansion, k is the thermal conductivity, θ is the temperature increment above the

reference absolute temperature T for the state of zero stress and strain, I_{yy} is the cross-sectional moment of inertia, A is the cross-sectional area, ρ is the density, K_x is the Timoshenko shear coefficient, t is time, u is the transverse deformation, h is the beam depth, q the input heat flux, s is the circumferential arc length along the beam section, x and y are rectangular coordinates in the transverse beam directions, z is the rectangular coordinate in the beam lengthwise direction, and

$$\beta_0 = \beta(1-2\nu) = E\alpha, \quad c_0 = c(1-\varepsilon) \quad (3)$$

$$\varepsilon = \frac{(3\lambda + 2\mu)^2 \alpha^2 T}{(\lambda + 2\mu)c}, \quad \tilde{\theta}_y = \int_A x \theta dA$$

where in λ and μ are Lamé's constants, c is the specific heat per unit volume, and ν is Poisson's ratio.

We assume that $I_{xy} = 0$, the beam is of unit width, has pinned ends and is at zero temperature so that the boundary conditions are

$$u(0, t) = u_{,zz}(0, t) = u(l, t) = u_{,zz}(l, t) = \tilde{\theta}_y(0, t) = \tilde{\theta}_y(l, t) = 0 \quad \text{for } z = 0, l; t > 0 \quad (4)$$

We assume that the beam is initially at rest with zero initial displacement and temperature so that the initial conditions are

$$u(z, 0) = u_{,t}(z, 0) = u_{,tt}(z, 0) = u_{,ttt}(z, 0) = \tilde{\theta}_y(z, 0) = 0 \quad \text{for } 0 \leq z \leq l; t = 0 \quad (5)$$

The solution to the initial-value problem presented by Eqs. (1, 4, and 5) is

$$u(z, t) = \frac{-2\beta_0 q K_x \mu}{\rho^2 I_{yy} c_0} \cdot \frac{h}{l} \sum_{n=1,3,5}^{\infty} \alpha_n (I_1 + I_2 + I_3) \sin \alpha_n z \quad (6)$$

where

$$I_1 = \frac{\omega_{r_1} - e^{-\omega_{i_1} t} (\omega_{i_1} \sin \omega_{r_1} t + \omega_{r_1} \cos \omega_{r_1} t)}{\omega_{r_1} \cdot \omega_{i_5} (\omega_{i_1}^2 + \omega_{r_1}^2) (\omega_{i_3}^2 + \omega_{r_3}^2)}$$

$$I_2 = - \left\{ \frac{e^{-\omega_{i_5} t} \omega_{r_1} - e^{-\omega_{i_1} t} [(\omega_{i_1} - \omega_{i_5}) \sin \omega_{r_1} t + \omega_{r_1} \cos \omega_{r_1} t]}{\omega_{r_1} \omega_{i_5} [(\omega_{i_1} - \omega_{i_5})^2 + (\omega_{r_1})^2] [(\omega_{i_3} - \omega_{i_5})^2 + (\omega_{r_3})^2]} \right\} \quad (7)$$

$$I_3 = \frac{1}{\omega_{r_1} \omega_{r_3} \{ (\omega_{i_3}^2 + \omega_{r_3}^2) [(\omega_{i_3} - \omega_{i_5})^2 + (\omega_{r_3})^2] \}^{1/2}} \times$$

$$\left[\sin(\omega_{r_3} t + \phi) \times \right.$$

$$\left\{ \frac{e^{-\omega_{i_1} t} [-(\omega_{i_1} - \omega_{i_3}) \sin(\omega_{r_1} - \omega_{r_3}) t - (\omega_{r_1} - \omega_{r_3}) \times \cos(\omega_{r_1} - \omega_{r_3}) t] + (\omega_{r_1} - \omega_{r_3}) e^{-\omega_{i_3} t}}{2[(\omega_{i_1} - \omega_{i_3})^2 + (\omega_{r_1} - \omega_{r_3})^2]} + \right.$$

$$\left. \frac{e^{-\omega_{i_1} t} [-(\omega_{i_1} - \omega_{i_3}) \sin(\omega_{r_1} + \omega_{r_3}) t - (\omega_{r_1} + \omega_{r_3}) \times \cos(\omega_{r_1} + \omega_{r_3}) t] + (\omega_{r_1} + \omega_{r_3}) e^{-\omega_{i_3} t}}{2[(\omega_{i_1} - \omega_{i_3})^2 + (\omega_{r_1} + \omega_{r_3})^2]} - \right.$$

$$\left. \frac{\cos(\omega_{r_3} t + \phi) \times \left\{ \frac{e^{-\omega_{i_1} t} [(\omega_{r_1} - \omega_{r_3}) \sin(\omega_{r_1} - \omega_{r_3}) t - (\omega_{i_1} - \omega_{i_3}) \times \cos(\omega_{r_1} - \omega_{r_3}) t] + (\omega_{i_1} - \omega_{i_3}) e^{-\omega_{i_3} t}}{2[(\omega_{i_1} - \omega_{i_3})^2 + (\omega_{r_1} - \omega_{r_3})^2]} - \right. \right.$$

$$\left. \left. \frac{e^{-\omega_{i_1} t} [(\omega_{r_1} + \omega_{r_3}) \sin(\omega_{r_1} + \omega_{r_3}) t - (\omega_{i_1} - \omega_{i_3}) \times \cos(\omega_{r_1} + \omega_{r_3}) t] + (\omega_{i_1} - \omega_{i_3}) e^{-\omega_{i_3} t}}{2[(\omega_{i_1} - \omega_{i_3})^2 + (\omega_{r_1} + \omega_{r_3})^2]} \right\}}{2[(\omega_{i_1} - \omega_{i_3})^2 + (\omega_{r_1} + \omega_{r_3})^2]} \right]$$

The transverse deflection has a final value

$$\lim_{t \rightarrow \infty} u(z, t) = - \frac{h \beta_0 q K_x \mu}{\rho^2 I_{yy} c_0} \cdot \frac{2}{l} \sum_{n=1,3,5}^{\infty} \alpha_n \left\{ \frac{1}{\omega_{i_5} (\omega_{i_1}^2 + \omega_{r_1}^2) (\omega_{i_3}^2 + \omega_{r_3}^2)} \right\} \sin \alpha_n z \quad (8)$$

In Eqs. (7) and (8) the roots of the secular equation to the first order of ε are¹

Received October 24, 1972; revision received March 8, 1973.

Index categories: Thermal Stresses; Heat Conduction; Structural Dynamic Analysis.

* Analytical Engineer, Applied Mechanics. Member AIAA.

† Formerly Assistant Professor of Mechanics, Rensselaer Polytechnic Institute, Hartford Graduate Center, Hartford, Conn.